JOURNAL OF MATERIALS SCIENCE 32 (1997) 3883–3889

The mechanical properties of friction welded aluminium-based metal–matrix composite materials

Y. ZHOU, J. ZHANG, T. H. NORTH, Z. WANG
Department of Metallurgy and Materials Science, University of Toronto, Ontario, Canada, M5S IA4

The optimum joining parameters for the friction joining of aluminium-based metal–matrix composite (MMC) materials are examined. The properties of MMC/MMC, MMC/alloy 6061 and alloy 6061/alloy 6061 joints are derived following detailed factorial experimentation. The mechanical properties of the joints are evaluated using a combination of notch tensile testing and also conventional tensile and fatigue testing. The frictional pressure has a statistically-significant effect on the notch tensile strength of joints produced in all base material combinations. The upset pressure has only a statistically-significant influence on the notch tensile strength properties of alloy 6061/alloy 6061 joints. The notch tensile strengths of MMC/alloy 6061 joints are significantly lower than MMC/MMC and alloy 6061/alloy 6061 joints for all joining parameter settings. The fatigue strength of MMC/MMC joints and alloy 6061/6061 joints are also poorer than the as-received base materials.

1. Introduction

The high specific strength and specific stiffness properties of aluminium-based metal matrix composite (MMC) base material compared with conventional aluminium-based alloys readily explains the driving force for the application of this material in the automotive and aerospace industries. Friction welding is a promising candidate for joining aluminium-based MMC base materials since joints can be made rapidly and consistently using this fabrication technique. The friction welding process can be considered as a series of sequential stages, namely: stage I where heat is generated by sliding friction and the torque reaches its maximum value; stage II where heat is generated by mechanical dissipation in the plasticized material and softened material flows radially outwards; stage III where a steady-state situation is attained and the torque, temperature distribution and rate of axial shortening (burn-off) are essentially constant; stage IV where the rotation is terminated and stage V where upsetting occurs. Although a considerable amount of work has been performed on the joining of metals only limited research has been published concerning the metallurgical and mechanical properties of friction welded composite base material [1–5].

Midling *et al.* [1] have examined the properties of friction welded joints in an AlSiMg (A357) alloy containing 10 vol % of SiC particles with a mean diameter of 20 μm. Friction welding did not promote segregation of SiC particulate material at the joint centreline and the heat-affected-zone (HAZ) region on either side of the bondline contained a uniform distribution of $FeSiAl_4$, Si and β-Mg_2Si precipitates. The friction joining operation did produce a softened heat-affected zone region in AlSiMg (A357-T6) base material and full recovery of the HAZ mechanical properties was achieved following post weld heat-treatment of the test joints. The heat-treatment applied consisted of a solution treatment at 535 °C followed by ageing at 160 °C for 10 h.

Dissimilar joining of particulate-containing base material was examined by Kreye and Reiner [2] and also by Aritoshi *et al.* [3]. Kreye and Reiner [2] have examined friction joining of a mechanically-alloyed aluminium alloy (Dispal) containing a fine dispersion of alumina and carbide particles. The tensile strengths of Dispal/Dispal and Dispal/carbon steel and Dispal/AISI 316Ti stainless steel dissimilar joints were similar (300 MPa). Aritoshi *et al.* [3] compared the friction welding characteristics of OFC (oxygen-free) Cu/Al and Cu–70 wt % W/Al joints and observed that the width of the transition (intermixed) region produced during the friction welding increased markedly when the high temperature flow strength of the Cu–W composite material decreased. They associated the higher tensile strength of Cu–70 wt % W/Al joints with the formation of a thin interdiffused region at the joint interface.

Since for automotive industry applications cost considerations generally preclude the application of a post weld heat-treatment following any joining operation, there has been considerable interest in methods for optimizing the mechanical properties of as-welded friction joints. Cola [4] and also Cola and Baeslack [5] have examined the relationship between joining parameter settings and the tensile and torsional strength properties of inertia friction welded alloy 6061 tubing containing 10 vol % Al_2O_3

0022–2461

particles. However, the presence of unbonded regions, excessive joint misalignment and failure to remove external and internal flash from completed joints severely compromized the analysis of their test results.

The present paper employs factorial experimentation to investigate the mechanical (notch tensile strength and fatigue strength) and metallurgical properties of friction welded aluminium-based metal matrix composite base material containing 10 vol % Al_2O_3 particles. The properties of MMC/MMC joints are compared with conventional aluminium alloy 6061/alloy 6061 and dissimilar MMC/alloy 6061 joints.

2. Experimental procedure

The test materials comprised of 19 mm diameter bars of aluminium-based metal matrix composite alloy 6061/Al_2O_3 (W6A.10A-T6) and a conventional aluminium alloy 6061-T6. The aluminium-based MMC base material contained 10 vol % of Al_2O_3 particles with an average particle size of about 10 μm. The nominal chemical composition of the base material was 0.28 wt % Cu, 0.6 wt % Si, 1 wt % Mg, 0.2 wt % Cr, balance aluminium.

Friction welding was performed using a direct-drive welding machine. The optimization of the joining parameters was investigated via detailed 2^3 factorial experimentation. The independent variables during the factorial experimentation were the friction pressure, the friction time and also the forging pressure during the MMC/MMC, MMC/alloy 6061 and alloy 6061/alloy 6061 joining. The settings of all the other joining parameters were held constant during the test programme. A detailed discussion of the factorial experimentation method has been presented elsewhere [6].

It has already been pointed out that conventional tensile and torsion testing of friction welded joints produces results that may not reflect the actual mechanical properties that exist at the joint interface [7, 8]. For example, the strength of the joint interface may exceed the strength of the softer substrate. Also, the tensile strength of the bondline region can be increased significantly in dissimilar joints as a result of rigid restraint (in this case deformation at the bondline is strongly affected by the mechanical properties of the adjoining substrates. Since the properties of similar and dissimilar joints are compared in the present paper, notched tensile testing is used to monitor the bondline mechanical properties. It should be noted that the peripheries of some test joints contained small unbonded zones and that the notch tensile test configuration (Fig. 1(a and b)) prevented these defects from compromizing the subsequent analysis of the factorial experimentation results.

Tensile and fatigue testing of MMC/MMC and alloy 6061/MMC joints were performed at room temperature using an MTS servo-hydraulic machine. The fatigue test specimens were held in wood-alloy grips during tension–compression fatigue testing ($R = -1$). (R is the stress ratio and is determined by the ratio of the minimum stress amplitude to the maximum stress amplitude: $R = \sigma_{min}/\sigma_{max}$ where

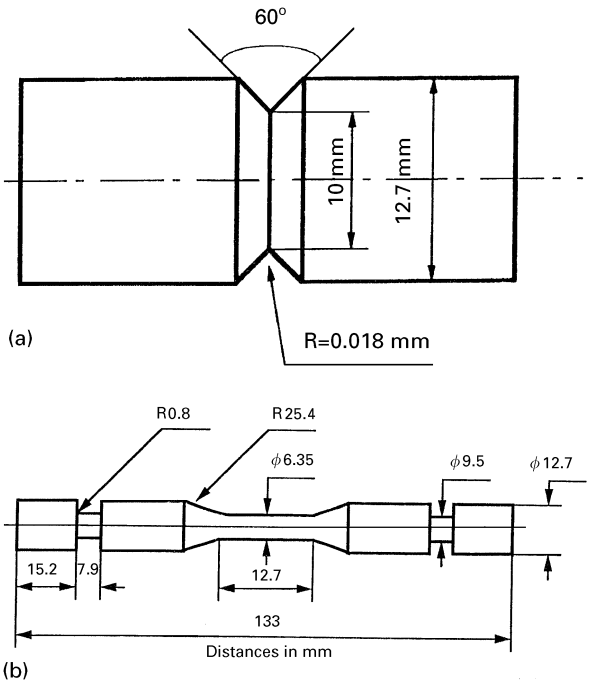

Figure 1 Design of (a) the notch tensile test specimen and (b) the fatigue test specimen.

σ_{min} is the minimum stress amplitude and σ_{max} is the maximum amplitude. The test frequency was 0.5 Hz and the selected stress values during the tests were determined following an examination of the tensile test results.The strain was measured using an MTS extensometer and the output results were collected and analysed using an IBM computer

3. Results and discussion

3.1. Joining parameters and optimum mechanical properties

The design matrix employed during the factorial experimentation and the corresponding mechanical response (notch tensile strength) are listed in Tables I–IV for the MMC/MMC, alloy 6061/alloy 6061 and MMC/alloy 6061 base material combinations. The regression equations that indicate the relationship between the joint mechanical properties and joining parameter settings for each base material combination are listed in Table V. The frictional pressure had a statistically-significant effect on the joint strength for all the investigated base material combinations. The upset pressure had only a statistically-significant effect on the notch tensile strength properties of the alloy 6061/alloy 6061 combination. For the range of the joining parameters investigated, varying the friction time had no effect on the joint notch tensile strength properties. It is worth noting that although the use of low frictional pressure values promoted the formation of unbonded regions at the outer peripheries of completed joints, the statistical analysis of joint mechanical properties was not confused by this particular problem.

The range of notch tensile strength values was relatively narrow in MMC/MMC, MMC/alloy 6061 and in alloy 6061/alloy 6061 joints. For example, the difference between the highest and lowest average notch

TABLE I Design matrix employed during factorial experimentation

Variables	Levels set for experiments			
	Low (−1)	High (1)	Base (0)	Interval
Frictional pressure, P_1 (MPa)	35	60	47.5	12.5
Frictional time, t_1 (s)	3	9	6	3
Forging pressure, P_2 (MPa)	35	90	62.5	27.5

TABLE II Notch tensile strength properties of MMC/MMC joints

Trial no.	Design matrix			Notch tensile strength (MPa)	
	P_1	t_1	P_2		Average
1	−1	−1	−1	293, 309	301
2	1	−1	−1	282, 342	312
3	−1	1	−1	300, 301	300
4	1	1	−1	315, 334	324
5	−1	−1	1	299, 316	307
6	1	−1	1	313, 314	313
7	−1	1	1	313, 319	316
8	1	1	1	327, 327	327

TABLE III Notch tensile strength properties of alloy 6061/alloy 6061 joints

Trial no.	Design matrix			Notch tensile strength (MPa)	
	P_1	t_1	P_2		Average
1	−1	−1	−1	283, 284, 307	291
2	1	−1	−1	295, 309, 317	307
3	−1	1	−1	276, 282, 289	282
4	1	1	−1	303, 304, 311	306
5	−1	−1	1	282, 287, 299	289
6	1	−1	1	314, 315, 320	316
7	−1	1	1	286, 299, 314	300
8	1	1	1	300, 315, 319	311

TABLE IV Notch tensile strength properties of dissimilar MMC/alloy 6061 joints

Trial no.	Design matrix			Notch tensile strength (MPa)	
	P_1	t_1	P_2		Average
1	−1	−1	−1	230, 263	246
2	1	−1	−1	222, 267	244
3	−1	1	−1	250, 257	253
4	1	1	−1	275, 278	276
5	−1	−1	1	240, 244	242
6	1	−1	1	284, 288	286
7	−1	1	1	233, 245	239
8	1	1	1	272, 296	284

tensile strength values was 27 MPa in MMC/MMC joints and 34 MPa in alloy 6061/alloy 6061 joints. In effect, there is a wide operating regime for the production of satisfactory joint strength properties when MMC base material is joined and in this respect, MMC/MMC and alloy 6061/alloy 6061 joints respond in a similar manner. The presence of reinforcing Al_2O_3 particles in the MMC base material readily explains the higher notch tensile strength properties of MMC/MMC joints compared with alloy 6061/alloy 6061 joints. However, the notched tensile strength of MMC/alloy 6061 joints had the lowest notch tensile strength values at all joining parameter settings (see Tables II–IV).

TABLE V Regression equations relating notch tensile strength with friction joining parameter settings. P_1 is the frictional pressure, P_2 is the upset pressure and t_1 is the friction time. (The statistically significant parameters are indicated in bold type)

Friction welded joints	Equations	Standard error
MMC/MMC	$312.75 + 6.5\boldsymbol{P_1} + 4.25t_1 + 3.25P_2$	3.59
MMC/alloy 6061	$259.0 + 13.75\boldsymbol{P_1} + 4.25t_1 + 3.75P_2$	4.52
Alloy 6061/alloy 6061	$300.4 + 9.75\boldsymbol{P_1} + 0.585t_1 + 3.75\boldsymbol{P_2}$	1.95

The optimum notch tensile strength in MMC/MMC, MMC/alloy 6061 and alloy 6061/alloy 6061 joints occurred when the frictional pressure and the upset pressure were set at their highest levels. Increasing the frictional pressure increases the burn-off rate and the equilibrium torque during the steady-state period (stage III) of the friction welding operation [9]. Also, increasing the frictional pressure (at a constant rotational speed) and decreasing the rotational speed (at constant frictional pressure) promotes spreading of the plastic zone across the whole joint interface. The steady-state temperature attained at the joint interface during friction welding is linearly related to the frictional energy supplied per unit volume of base material [10]. Assuming that all axial shortening (burn-off) during the joining operation occurs at the joint interface, then the frictional energy applied at the contact region can be given by the following expression:

$$\text{Frictional energy per unit volume} = \frac{9.803 \times 10^{-3} P_1 V_h + 1.027 \times 10^{-3} N T_{ST}}{A V_h} \quad (1)$$

where, P_1 is the friction pressure (kg mm^{-2}), V_h is the burn-off rate (mm s^{-1}), N is the rotational speed (rpm), T_{st} is the steady torque (kgm) and A is the area of the base metal (mm^2).

The frictional energy per unit volume is therefore maximized when a high frictional pressure is used and this produces joints with the highest notch tensile strength properties. It is worth noting that Shinoda *et al.* [11] have reported that the highest strength in friction welded aluminium alloy A5056-H32 joints occurred when the highest energy input was applied during the friction joining.

Fig. 2 shows examples of the softened heat-affected-zone region produced on either side of the joint interface in friction welded MMC/MMC and alloy 6061/alloy 6061 base materials. Heat-affected-zone region softening has been associated with solution and over-ageing of precipitates in the as-received base

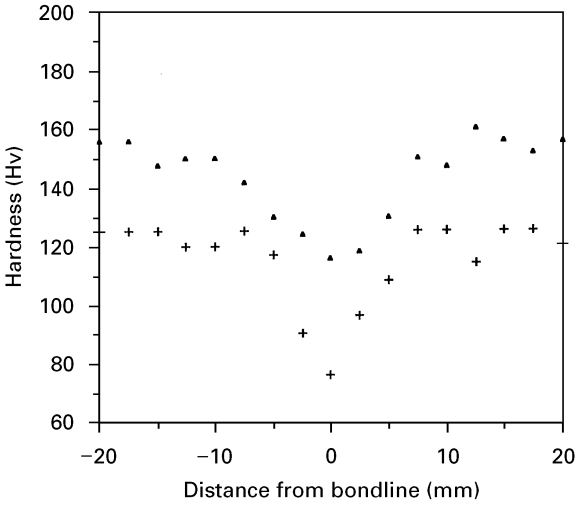

Figure 2 Heat-affected-zone softening in (▲) MMC/MMC and (+) alloy 6061/alloy 6061 joints.

material [1]. In the present study, the width of the softened HAZ region decreased when high friction pressure values were applied.

3.2. Dissimilar joint properties

The joint interface profile produced during dissimilar MMC/alloy 6061 joining is quite different to that in MMC/MMC joints. Wedge-shaped islands comprizing alumina particles entrained in alloy 6061 substrate material were observed adjacent to the joint interface near the periphery of the dissimilar MMC/alloy 6061 joints (see Fig. 3). The mechanism of formation of these entrainment regions can be explained by the following arguments. When the substrates contact each other, the initial stage of the friction welding operation (stage I) is characterized by the production of a large number of localized adhesion/seizure/shearing events [9]. These localized adhesion/seizure/shearing events transfer material from one substrate to the other and *vice-versa*. The steady-state period (stage III) of friction welding is characterized by the formation of a fully-plasticized region and the torque, temperature and rate of axial shortening are essentially constant. In dissimilar joints the interface profile will be determined by the relative mechanical properties (shear stress) at high temperature of the two substrates. The joint interface profile formed in alloy 6061/MMC joints is concave in the lower strength (alloy 6061) substrate since it has the lowest high temperature shear stress (see Fig. 4a). When the flow stresses of the dissimilar substrates are significantly different there is negligible plastic deformation in the higher strength substrate. This readily explains the planar joint interface profile formed when MMC base material is friction welded to AISI 304 stainless steel (see Fig. 4b).

Friction joining is characterized by very high strain rates and severe plastic deformation of the contacting substrates. For example, the calculated strain rate in the contact zone is as high as $10^4\,s^{-1}$ during the friction welding of AlSiMg (A357) alloy base material [12]. Also, the strain rate markedly varies across the joint region and the joining process is characterized by

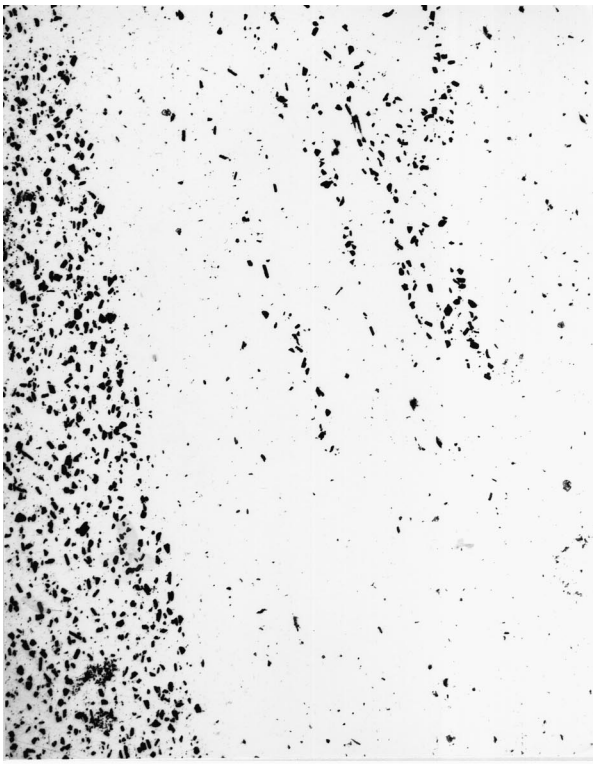

Figure 3 Entrainment of MMC base material in the alloy 6061 matrix adjacent to the joint interface (magnification × 80).

a non-uniform plastic flow and fracture of particulate material [13]. Many fractured alumina particles were observed in the wedge-shaped islands of entrained MMC material adjacent to the MMC/alloy 6061 joint interface (see Fig. 5). Also, there was clear evidence of disbonding between the alumina particles and the surrounding matrix (see Fig. 5). The MMC entrainment regions were located at the root of the machined notches in the notched tensile test specimens. As a result, the poorer notch tensile strength properties of dissimilar MMC/alloy 6061 joints (see Table IV) can be partially explained by preferential test specimen failure promoted by particle fissuring and particle/matrix disbonding in MMC entrainment regions immediately ahead of the notch tip. In addition, the friction welding process *per se* promotes particle segregation in localized regions at the bondline. Fig. 6 shows preferential segregation of closely-spaced, small diameter alumina particles in an MMC/alloy 6061 test sample. The lower notch tensile strength of MMC/alloy 6061 joints, therefore, may also be the result of preferential failure through localized regions of particle segregation at the bondline.

3.3. Notch tensile strengths of base material and joint regions

Table VI compares the tensile strength properties of as-received MMC and alloy 6061 base materials and friction welded joints. Both conventional tensile and notch tensile testing indicate that the joint regions have lower strengths than the as-received base material. The lower strength of the alloy 6061/alloy 6061 friction welds results from the presence of softened heat-affected-zone regions on either side of the

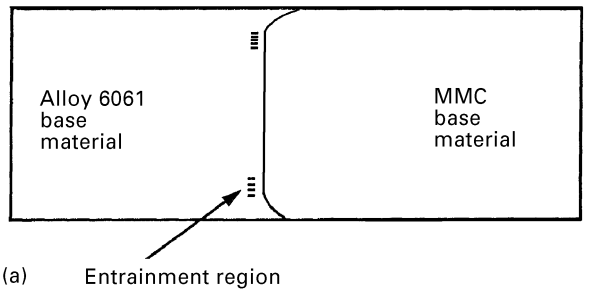

Figure 4a Schematic showing the curved joint interface region and the location of entrainment regions in the dissimilar MMC/alloy 6061 joints.

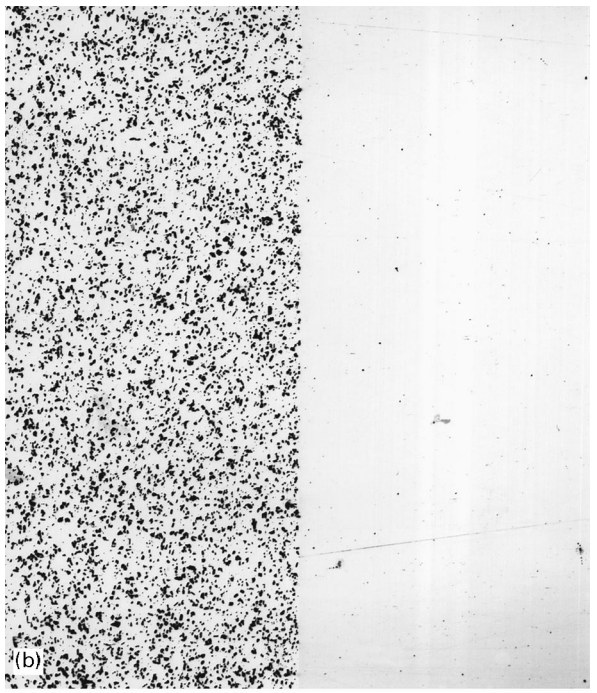

Figure 4b Planar joint interface produced in dissimilar MMC/AISI 304 stainless steel joints (magnification × 40).

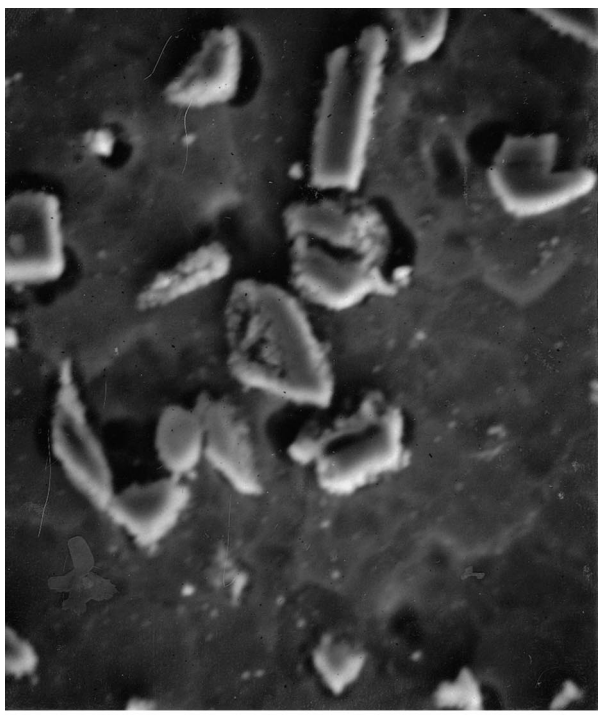

Figure 5 Fractured alumina particles and particle/matrix disbonding in the MMC entrainment region adjacent to the joint interface in MMC/alloy 6061 joints (magnification × 1050).

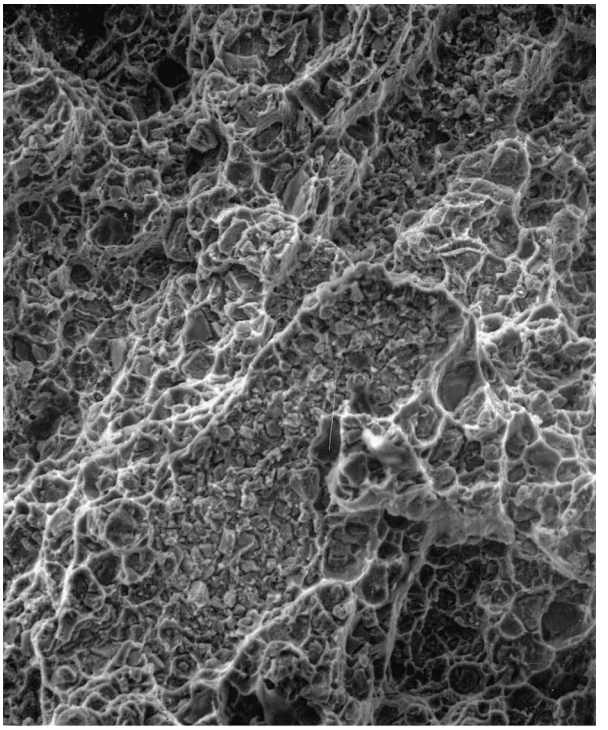

Figure 6 Localized segregation of closely-spaced, small diameter alumina particles on the fracture surface of an MMC/alloy 6061 joint (magnification × 220).

TABLE VI Tensile strength of MMC and alloy 6061 base materials and friction welded joints

	Notch tensile strength (MPa)	Ultimate tensile strength[a] (MPa)
MMC base material	460	354
MMC/MMC friction joints	308	257
Alloy 6061 base material	447	299
Alloy 6061/alloy 6061 friction joints	299	190

[a] Ultimate strength found during conventional tensile testing

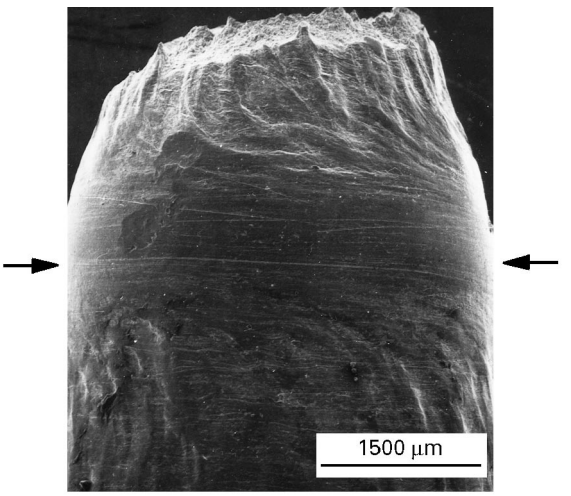

Figure 7 Tensile failure in the softened heat-affected-zone region of an alloy 6061/alloy 6061 joint (the arrows show the location of the joint interface).

bondline (see Fig. 7). In MMC/MMC joints, tensile failure occurred at the joint interface and the fracture surfaces of broken test specimens exhibited clear indications of the spiral deformation produced by the friction welding operation.

3.4. Fatigue strength properties

Figs 8 and 9 show the fatigue life curves of the MMC and alloy 6061 base materials and the respective joint regions. It is important to point out that these results were obtained using low cycle fatigue testing where the principal aim was to determine the mode of fatigue failure of friction welded joints. As can be seen from these figures, the friction welded joints had markedly poorer fatigue strengths than the as-received base materials. Table VII indicates the 95% confidence limits of the fatigue strength at 10^5 fatigue cycles. The

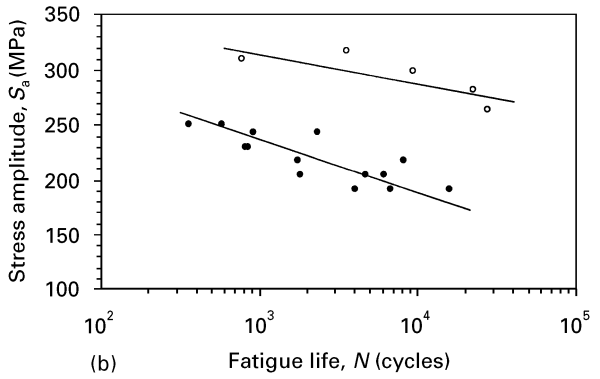

Figure 8 Fatigue strength of: (○) as-received MMC base material and (●) MMC/MMC joint regions.

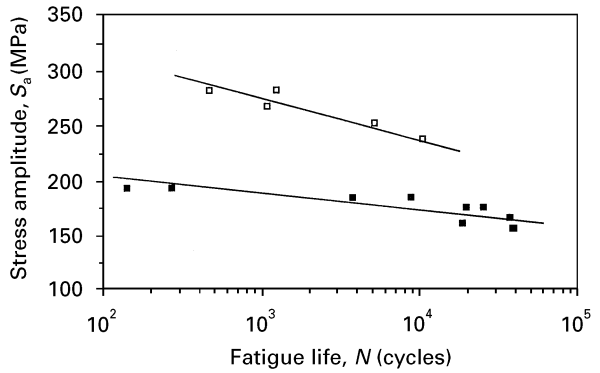

Figure 9 Fatigue strength of: (□) as-received alloy 6061 base material and (■) alloy 6061/alloy 6061 joint regions.

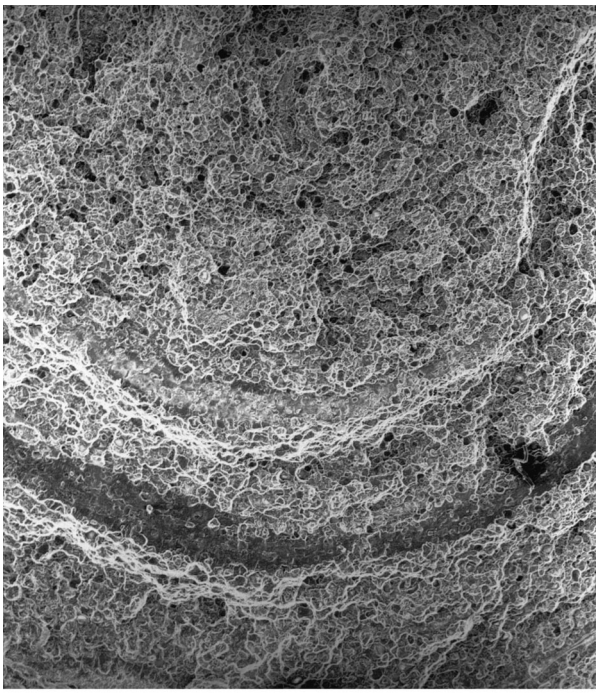

Figure 10 Fatigue failure in an MMC/MMC joint showing evidence of spiral deformation on the fracture surface (magnification × 24).

median fatigue strengths of MMC/MMC and alloy 6061/alloy 6061 joints were 54 and 32% lower than the as-received base materials. A preliminary study has demonstrated that the fatigue failure was initiated in the softened heat-affected-zone region for alloy 6061/alloy 6061 joints whereas in MMC/MMC joints it was initiated at the bondline region. Evidence for this conclusion is the spiral deformation observed on the fracture surface of failed MMC/MMC joints (see Fig. 10). Following fracture initiation at the bondline, the remainder of the fatigue test specimen fractured in regions away from the joint interface.

4. Conclusions

The influence of joining parameter settings on the mechanical and metallurgical properties of MMC/MMC, MMC/alloy 6061 and alloy 6061/alloy 6061 base materials has been investigated using factorial experimentation. It has been confirmed that:

(1) The frictional pressure had a statistically-significant effect on the notch tensile strength of MMC/MMC, MMC/alloy 6061 and alloy 6061/alloy 6061

TABLE VII 95% confidence limits of fatigue strength at 10^5 cycles for the as-received base materials and welded joints

Material	Upper confidence limit (MPa)	Median value (MPa)	Lower confidence limit (MPa)
Alloy 6061 base material	241.5	200.5	159.5
Alloy 6061/alloy 6061 joint	167.8	137.1	106.3
MMC base material	300.1	247.9	195.8
MMC/MMC joint	161.7	114.9	68.2

joints. The upset pressure had only a statistically-significant effect on the notch tensile strength properties of the alloy 6061/alloy 6061 joints. For the range of joining parameters investigated, varying the friction time had no significant effect on the notch tensile strength of joint regions.

(2) The notch tensile strength of MMC/alloy 6061 joints were lower than MMC/MMC and alloy 6061 /alloy 6061 joints for all the investigated joining parameter settings. The lower notch tensile strength properties of dissimilar MMC/alloy 6061 joints can be explained by (a) preferential failure caused by fractured particles and particle/matrix disbonding in MMC entrainment regions immediately ahead of the notch tip, and (b) the formation of localized regions of particle segregation at the joint interface.

(3) The fatigue life of friction welded joints was poorer than in as-received base material. In alloy 6061/alloy 6061 joints, fatigue failure initiated in the softened heat-affected-zone region. In MMC/ MMC joints, fatigue failure initiated at the bondline region.

Acknowledgement

The authors wish to acknowledge the financial support provided by the Ontario Centre for Materials Research (OCMR) for this research programme. The authors also wish to acknowledge support of Alcan International, Kingston who supplied the base material and also detailed technical discussions.

References

1. O. T. MIDLING, O. GRONG and M. CAMPING, in Proceedings of the 12th Int. Symp. on Metallurgy and Materials Science, Riso, edited by N. Hansen (Riso National Laboratory, Denmark, 1991) pp. 529–534.
2. H. KREYE and G. REINER, in Proceedings of the ASM Conference on Trends in Welding Research, Gatlinburg, TN, May 1986 edited by S. David and J. Vitek (ASM International Metals Park, 1986) p. 728–731.
3. M. ARITOSHI, K. OKITA, T. ENDO, K. IKEUCHI and F. MATSUDA, *Jpn. Weld. Soc.* **8** (1977) 50.
4. M. J. COLA, M.A.Sc thesis, Ohio State University, OH (1992).
5. M. J. COLA and W. A. BAESLACK, in Proceedings of the 3rd Inter. SAMPE Conf., Toronto Oct., 1992, edited by D. H. Froes, W. Wallace, R. A. Cull, and E. Struckholt, Vol. 3, p. M424–438.
6. K. K. WANG and G. RASMUSSEN, *Trans. ASME* **9** (1972) 999.
7. T. J. JESSOP and W. O. DINSDALE, in Proceedings of Advances in Welding Processes, Harrogate 1978 (The Welding Institute, Cambridge, UK) pp. 23–36.
8. A. FUJI, T. H. NORTH, K. AMEYAMA and M. FUTAMATA, *Mater. Sci. Tech.* **3** (1992) 219.
9. F. D. DUFFIN and A. S. BAHRANI, *Metal Const.* **5** (1973) 125.
10. K. OKITA and M. ARITOSHI, *Trans. Jpn. Weld. Soc.* **13** (1982) 9.
11. T. SHINODA, K. TANADA, Y. KATOH and T. SHIMIZU, *Weld. Int.* **8** (1994) 349.
12. O. MIDLING and O. GRONG, *Acta Metall. Mater.* **42** (1994) 1595.
13. Y. ZHOU, Z. LI, L. HU, A. FUJI and T. H. NORTH, *ISIJ Jpn. Int.* **35** (1995) 1315–1321.

Received 21 March 1995
and accepted 21 October 1996